Influence of ocular chromatic aberration and pupil size on transverse resolution in ophthalmic adaptive optics optical coherence tomography

Enrique J. Fernández

Center for Biomedical Engineering and Physics, Vienna University of Medicine, Austria
Laboratorio de Optica, Department of Physics, University of Murcia, Spain
enrique.fernandez@meduniwien.ac.at

Wolfgang Drexler

Center for Biomedical Engineering and Physics, Vienna University of Medicine, Austria
wolfgang.drexler@meduniwien.ac.at

Abstract: Optical coherence tomography (OCT) enables visualization of the living human retina with unprecedented high axial resolution. The transverse resolution of existing OCT approaches is relatively modest as compared to other retinal imaging techniques. In this context, the use of adaptive optics (AO) to correct for ocular aberrations in combination with OCT has recently been demonstrated to notably increase the transverse resolution of the retinal OCT tomograms. AO is required when imaging is performed through moderate and large pupil sizes. A fundamental difference of OCT as compared to other imaging techniques is the demand of polychromatic light to accomplish high axial resolution. In ophthalmic OCT applications, the performance is therefore also limited by ocular chromatic aberrations. In the current work, the effects of chromatic and monochromatic ocular aberrations on the quality of retinal OCT tomograms, especially concerning transverse resolution, sensitivity and contrast, are theoretically studied and characterized. The repercussion of the chosen spectral bandwidth and pupil size on the final transverse resolution of OCT tomograms is quantitatively examined. It is found that losses in the intensity of OCT images obtained with monochromatic aberration correction can be up to 80 %, using a pupil size of 8 mm diameter in combination with a spectral bandwidth of 120 nm full width at half maximum for AO ultrahigh resolution OCT. The limits to the performance of AO for correction of monochromatic aberrations in OCT are established. The reduction of the detected signal and the resulting transverse resolution caused by chromatic aberration of the human eye is found to be strongly dependent on the employed bandwidth and pupil size. Comparison of theoretical results with experimental findings obtained in living human eyes is also provided.

OCIS codes: (170.4500) Optical coherence tomography; (010.1080) Adaptive optics; (330.4460) Ophthalmic optics; (110.2990) Image formation theory; (350.5730) Resolution; (220.1000) Aberration compensation; (330.5370) Physiological optics.

References and links

1. D. Huang, E. A. Swanson, C. P. Lin, J. S. Schuman,W. G. Stinson, W. Chang, M. R. Hee, T. Flotte, K. Gregory, C. A. Puliafito, and J. G. Fujimoto, "Optical coherence tomography," Science **254**, 1178-1181 (1991).
2. W. Drexler, U. Morgner, R. K. Ghanta, F. X. Kärtner, J. S. Schuman, and J. G. Fujimoto, "Ultrahigh-resolution ophthalmic optical coherence tomography," Nature Medicine **7**, 502-507 (2001).
3. W. Drexler, U. Morgner, F. X. Kärtner, C. Pitris, S. A. Boppart, X. D. Li, E. P. Ippen, and J. G. Fujimoto, "In vivo ultrahigh-resolution optical coherence tomography," Opt. Lett. **24**, 1221-1223 (1999).

#8582 - $15.00 USD Received 25 August 2005; revised 23 September 2005; accepted 23 September 2005

4. W. Drexler, "Ultrahigh resolution optical coherence tomography," J. Biomed. Opt. **9**, 47-74 (2004).
5. A. Unterhuber, B. Povazay, B. Hermann, H. Sattmann, W. Drexler, V. Yakovlev, G. Tempea, C. Schubert, E. M. Anger, P. K. Ahnelt, M. Stur, J. E. Morgan, A. Cowey, G. Jung, T. Le, and A. Stingl, "Compact, low-cost TiAl2O3 laser for in vivo ultrahigh-resolution optical coherence tomography," Opt. Lett. **28**, 905-907 (2003).
6. J. Porter, A. Guirao, I. G. Cox, and D. R. Williams, "Monochromatic aberrations of the human eye in a large population," J. Opt. Soc. Am. A **18**, 1793–1803 (2001).
7. L. N. Thibos, X. Hong, A. Bradley, and X. Cheng, "Statistical variation of aberration structure and image quality in a normal population of healthy eyes," J. Opt. Soc. Am. A **19**, 2329-2348 (2002).
8. F. J. Castejón-Mochón, N. López-Gil, A. Benito, and P. Artal, "Ocular wavefront aberration statistics in a normal young population," Vis. Res. **42**, 1611–1617 (2002).
9. E. J. Fernández, I. Iglesias, and P. Artal, "Closed-loop adaptive optics in the human eye," Opt. Lett. **26**, 746-748 (2001).
10. H. Hofer, L. Chen, G. Y. Yoon, B. Singer, Y. Yamauchi, and D. R. Williams, "Performance of the Rochester 2nd generation adaptive optics system for the eye," Opt. Express **8**, 631–643 (2001), http://www.opticsexpress.org/abstract.cfm?URI=OPEX-8-11-631.
11. A. Roorda, F. Romero-Borja, W. J. Donnelly III, H. Queener, T. J. Hebert, and M. C. W. Campbell, "Adaptive optics scanning laser ophthalmoscopy," Opt. Express **10**, 405-412 (2002), http://www.opticsexpress.org/abstract.cfm?URI=OPEX-10-9-405.
12. D. T. Miller, J. Qu, R. S. Jonnal, and K. Thorn, Coherence gating and adaptive optics in the eye. In: V. V. Tuchin, J. A. Izatt, and J. G. Fujimoto (Eds.), Coherence Domain Optical Methods and Optical Coherence Tomography in Biomedicine VII, Proc. SPIE **4956**, 65-72 (2003).
13. B. Hermann, E. J. Fernández, A. Unterhuber, H. Sattmann, A. F. Fercher, W. Drexler, P. M. Prieto, and P. Artal, "Adaptive optics ultrahigh resolution optical coherence tomography," Opt. Lett. **29**, 2142-2144 (2004).
14. E. J. Fernández and P. Artal, "Membrane deformable mirror for adaptive optics: performance limits in visual optics," Opt. Express **11**, 1056-1069 (2003), http://www.opticsexpress.org/abstract.cfm?URI=OPEX-11-9-1056.
15. Y. Zhang, J. Rha, R. S. Jonnal, and D. T. Miller, "Adaptive optics spectral optical coherence tomography for imaging the living retina," Opt. Express **13**, 4792-4811 (2005), http://www.opticsexpress.org/abstract.cfm?URI=OPEX-13-12-4792.
16. E. J. Fernández, B. Povazay, B. Hermann, A. Unterhuber, H. Sattmann, P. M. Prieto, R. Leitgeb, P. Ahnelt, P. Artal, and W. Drexler, "Three Dimensional Adaptive Optics Ultrahigh-Resolution Optical Coherence Tomography using a liquid crystal spatial light modulator," Vis. Res. In press (2005)
17. E. J. Fernández, A. Unterhuber, P. M. Prieto, B. Hermann, W. Drexler, and P. Artal, "Ocular aberrations as a function of wavelength in the near infrared measured with a femtosecond laser," Opt. Express **13**, 400-409 (2005), http://www.opticsexpress.org/abstract.cfm?URI=OPEX-13-2-400.
18. S. Kimura and T. Wilson, "Confocal scanning optical microscope using single-mode fiber for signal detection," App. Opt. **30**, 2143-2150 (1991).
19. T. Wilson, Ed., *Confocal Microscopy* (Academic, London, 1990).
20. T. Wilson and A. R. Carlini, "Size of the detector in confocal imaging systems," Opt. Lett. **12**, 227-229 (1987).
21. A. G. Podoleanu and D. A. Jackson, "Noise analysis of a combined optical coherence tomograph and a confocal scanning ophthalmoscope," Appl. Opt. **38**, 2116-2127 (1999).
22. A. G. Podoleanu, G. M. Dobre, R. G. Cucu, and R. B. Rosen, "Sequential optical coherence tomography and confocal imaging," Opt. Lett. **29**, 364-366 (2004).
23. D. A. Atchinson and G. Smith, *Optics of the Human Eye* (Oxford: Butterworth-Heinemann, 2000).
24. A. G. Bennett and R. B. Rabbetts, *Clinical Visual Optics* (Butterworth-Heinemann, Oxford, 1998).
25. T. Wilson and C. J. R. Sheppard, *Theory and Practice of Scanning Optical Microscopy* (Academic press, London,1984).
26. P. Artal, S. Marcos, R. Navarro, and D. R. Williams, "Odd aberrations and double-pass measurements of retinal image quality," J. Opt. Soc. Am. A **12**, 195–201 (1995).
27. M. Born and E. Wolf, *Principles of Optics* (7th ed., Pergamon, Oxford, 1999).
28. W. S. Stiles, "The luminous efficiency of rays entering the eye pupil at different points," Proc. R. Soc. London, Ser. B **112**, 428-450 (1933).
29. A. van Meeteren, "Calculations on the optical modulation function of the human eye for white light," Opt. Acta **21**, 395-412 (1972).
30. P. Artal, "Incorporation of directional effects of the retina into computations of the modulation transfer function of human eyes," J. Opt. Soc. Am. A **6**, 1941-1944 (1989).
31. R. J. Noll, "Zernike polynomials and atmospheric turbulence," J. Opt. Soc. Am. **66**, 207 211 (1976).

#8582 - $15.00 USD Received 25 August 2005; revised 23 September 2005; accepted 23 September 2005

1. Introduction

Optical coherence tomography (OCT) is a well established non-invasive, cross-sectional imaging modality based on white light interferometry [1]. The use of OCT in the living human eye enables visualization of intraretinal layers with unprecedented axial resolution [2]. In particular, ultrahigh resolution OCT (UHR OCT) [2-4] permits up to 2-3 μm of axial resolution in the living retina by employing mode-locked Titanium:sapphire pulsed laser sources, emitting smooth, ultrabroad bandwidth spectra in the near infrared range of up to 170 nm [5]. In low coherence interferometry, axial resolution is mainly governed by the spectral bandwidth of the light source, while transverse resolution is given by the optical quality of the refractive system. The ability to focus the light in a concentrated, small and bright spot onto the retina finally governs transverse resolution, contrast and sensitivity of the optical imaging system. In ophthalmic OCT, the eye is the effective objective of the imaging system, and also the main source of aberrations. Ocular aberrations are known to increase with pupil size. Even in normal eyes, ocular aberrations notably degrade the optical quality of retinal images for pupil diameters larger than 1.5-2 mm [6-8]. However, keeping the pupil small prevents high transverse resolution, because of the reduced numerical aperture. The most common pupil size used in ophthalmic OCT systems so far is 1-1.5 mm diameter. A possible approach to increase transverse resolution is to expand the pupil and beam diameter, enlarging the effective numerical aperture at the eye's pupil. Simultaneously, aberration correction is then required in order to keep a reasonable optical quality of the eye. In this context, adaptive optics has been successfully demonstrated to measure and correct ocular aberration in the human eye in real time [9,10]. Several ophthalmic imaging techniques currently benefit from AO, e.g. scanning laser ophthalmoscopy [11] and flood illumination cameras [10]. The combination of AO and OCT was first proposed for en face OCT imaging with standard axial resolution [12]. The successful combination of AO with UHR OCT was demonstrated for the first time, achieving improved transverse resolution (~5-10 μm) compared to ~20 μm accomplished so far [13] using an electrostatic deformable mirror [14]. Other attempts to interface AO, using a different type of deformable mirror, and OCT have recently been reported [15]. The benefits of AO for three dimensional UHR OCT retinal imaging have also recently been demonstrated using a liquid crystal spatial light modulator as correcting device, increasing transverse resolution to 5 μm by maintaining 2-3 μm axial resolution [16].

A fundamental difference in OCT compared to other ophthalmic imaging techniques is the mandatory requirement of polychromatic light sources to accomplish high axial resolution. Hence, the benefits of using AO can not directly be compared to the other monochromatic retinal imaging techniques mentioned above. The effective repercussion of monochromatic aberrations in the final retinal OCT tomogram quality, in particular concerning transverse OCT tomogram resolution, using polychromatic light sources has not been studied so far. The presence of chromatic aberrations in the eye, recently characterized in the near infrared in normal human eyes [17], adds an additional important factor in the analysis of the performance of AO UHR OCT. The possible expansion of the eye's pupil size used to image the retina with improved transverse resolution, simultaneously introduces the effects of chromatic aberration. Usually chromatic aberrations are divided in two different parts: the transverse and the longitudinal chromatic aberration (TCA and LCA respectively). Although the distinction is not based in physical arguments, because the origin of both chromatic aberrations is exactly the same, the latter classification might be useful in some practical situations. TCA normally refers to the change in position and magnification of extended images produced onto the retina, as a function of wavelength. TCA exhibits a huge variability among subjects. The interest of TCA is rather limited for AO UHR OCT, where a beam is scanned at the eye's entrance pupil producing near to point images onto the retina. Consequently, this aberration will not be considered in the present work. LCA is associated with variations of the effective focus plane of different images, as a function of wavelength. The range of LCA only shows minor variations among subjects. In this work, the effects of both LCA and monochromatic aberrations determining the optical quality of OCT tomograms

#8582 - $15.00 USD Received 25 August 2005; revised 23 September 2005; accepted 23 September 2005

will be studied by simulating the effective point images projected onto the detector during OCT signal acquisition. The benefits of AO, correcting monochromatic aberrations, will be established. In this context, the effective transverse resolution in the OCT images will be investigated quantitatively. The effect of employing different spectral bandwidths will be studied over the whole range of possible pupil sizes possible in the human eye.

2. Methods

2.1. Fiber optical based ophthalmic OCT

The majority of the ophthalmic OCT setups are fully fiber optical based, notably simplifying alignment of the interferometer and enabling portable and reliable instruments for clinical use. In this approach, signals coming from the sample and the reference arm interfere in a fiber coupler, to be sequentially recorded at the detector. Appropriate fiber collimating lenses are necessary to launch the light onto the sample or the mirror in the reference arm as well as to efficiently couple light reflected from the sample back into the fiber. Single-mode optical fibers are generally used on ophthalmic OCT, with core diameters in the order of 3-5 μm for cut-off wavelengths of 630-850 nm. In these systems, light is emitted and collected by the same effective pinhole, which is the core diameter of the fiber.

Given a particular fiber core diameter, the use of certain collimators, with appropriated numerical apertures, reproduces the confocal behavior found in classical confocal microscopes, where pinholes are located in front of the detector. The use of single-mode fiber as a detector in microscopy has previously been reported [18]. The optical performance of confocal systems [19] as well as the effects of pinhole size on both transverse and axial resolution has been also studied [20]. The similarities between fiber-based OCT systems and confocal microscopy have been considered and experimentally implemented in the human eye, showing the benefits of the combination of both techniques [21,22].

The assumption of confocal detection when using a single-mode fiber [18] is mainly governed by the normalized radius of the fiber:

$$R = \frac{2\pi}{\lambda} r \sin(\alpha), \tag{1}$$

where r is the core of the optical fiber, λ is the considered wavelength and sin(α) corresponds to the numerical aperture. For an ideal confocal point detector, the normalized radius is zero. Under certain conditions the sample arm apparatus in ophthalmic OCT systems can be considered as a confocal scanning detector. In practice, the numerical aperture of the collimating lens placed in front of the fiber can be chosen appropriately, making possible to mathematically assume the normalized radius as practically zero. In the current work, the transverse resolution of a fiber optical based ophthalmic OCT system will be studied theoretically, assuming confocal detection.

2.2. Ocular aberrations

In a well designed OCT setup, the eye is the main source of wavefront aberrations. Monochromatic ocular aberrations, excluding defocus, are known to be practically independent of wavelength in the near infrared [17]. Hence, in this work they will be assumed to be constant. LCA in the eye has been mathematically modeled [17] in the near infrared as:

$$ChromaticDefocus = 0{,}0021(\lambda - 800), \tag{2}$$

where λ is the wavelength in nanometers. This expression gives the chromatic defocus in diopters, taking a wavelength of 800 nm as the reference. It will be used for the rest of this work to simulate ocular chromatic aberration. The central wavelength in many light sources currently used for OCT retinal imaging is around 800 nm, supporting the use of this particular value as a reference.

#8582 - $15.00 USD Received 25 August 2005; revised 23 September 2005; accepted 23 September 2005

The influence of monochromatic aberrations on the performance of the OCT setup will be studied by using objective measurement obtained in four normal and young subjects at 800 nm. Aberrations were recorded by means of a Hartmann-Shack wavefront sensor. The measurements and the details of the procedure are explained elsewhere [17].

In order to evaluate the size of the retinal images, it is necessary to make some assumptions on the dimensions and optical parameters of the eye. A simple eye model, the Emsley's version, will be adopted [23,24]. It consists of a single convex surface separating air from a medium of refractive index similar to that of the vitreous with a refractive index of 1.33. In this model, the total power of the eye is 60 D. Therefore, the focal length is 22.22 mm and the radius of curvature of the first surface is 5.56 mm. The principal points coincide with the vertex of the refracting surface. For simplicity, the entrance and exit pupils are assumed at the principal planes.

2.3. Point spread function of the sample arm

Under the previously discussed conditions, the sample arm of the interferometer in a fiber optical based ophthalmic OCT system operates as a confocal detector. In confocal microscopy, the image of a point object is given by the general expression [25]:

$$I = \left|PSF_1\right|^2 \left\{ \left|PSF_2\right|^2 \otimes D \right\}, \tag{3}$$

where PSF_1 is the point spread function (PSF) of the optical system used to illuminate the sample, and PSF_2 corresponds to the optical system responsible for the detection of light reflected or transmitted from the sample. The symbol $\otimes$ indicates convolution operation. D is the intensity sensitivity, which in the case of perfect confocal detection can be mathematically described by a Dirac delta function. In this case, the effective PSF of the system is the square modulus of the product of the two *PSF*i. Moreover, in the case of a symmetrical system, where illumination and measurement are performed through the same optical apparatus, as it is done in ophthalmic OCT, the image of a point is proportional to the square of the PSF_1 of the system in a single pass.

The single pass PSF can be obtained by squaring the complex amplitude of the electrical field [26,27]:

$$PSF_i(\lambda,\rho) \propto \left(\frac{1}{\lambda}\right)^2 \left| \iint_{Ai} J_0(2\pi\rho r)\, \xi(\lambda,r) \exp\left[i\, 2\pi \Phi(\lambda,r)\right] r dr \right|^2 . \tag{4}$$

The term $J_0(2\pi\rho r)$ is the Bessel function of first class, and first order. The function $\xi(\lambda,r)$ is the amplitude pupil transmission. This function could be used to model the Stiles-Crawford effect [28]. Previous works have demonstrated that the Stiles-Crawford effect has a modest impact in the estimation of the retinal image quality [29,30]. Consequently, in the present work, the amplitude pupil transmission will be assumed to be constant. The function $\Phi(\lambda,r)$ describes the ocular aberrations on the eye's exit pupil of area A_i. The ocular aberrations are described using the Zernike polynomials [27,31] up to the fifth order:

$$\Phi(\lambda,r) = \sum_{i=1}^{21} a_i Z_i , \tag{5}$$

where a_i represents the coefficient associated with the polynomial Z_i. All the coefficients are assumed to be independent of the considered wavelength, except for that associated with the defocus, which incorporates the LCA. Hence, the explicit expression for this particular term as a function of the radius r and wavelength λ is:

$$a_4 = -\left(\frac{r^2}{4\sqrt{3}}\right) 0.0021(\lambda - 800). \tag{6}$$

#8582 - $15.00 USD Received 25 August 2005; revised 23 September 2005; accepted 23 September 2005

The estimation of the single pass polychromatic PSF at a given pupil size can be obtained by integrating all the contribution from the different wavelengths:

$$PSF_{Polychromatic} = \frac{1}{\mathrm{K}}\frac{1}{\mathrm{M}}\int_{-\infty}^{+\infty} PSF_i(\lambda,\rho)G(\lambda)d\lambda\,. \tag{7}$$

G(λ) is the Gaussian function describing the spectral distribution of the illuminating light, resembling the situation of an ideal light source for OCT retinal imaging. Other possible spectral shapes can be easily incorporated in the calculations by appropriately changing the function G. Five different cases are considered in the present study, corresponding to Gaussian spectra of 40, 80, 120, 160 and 200 nm bandwidth of full width at half maximum (FWHM), all of them centered at 800 nm. In order to compare polychromatic PSFs among different bandwidth the normalizing constant K is introduced. The normalization forces the maximum of each PSF to be constant in the perfect case, independently of the considered bandwidth, when no aberrations are present. The parameter M allows comparison among images obtained at different pupil sizes, from 1 to 8 mm diameter, also normalizing the maximum energy projected onto the retina in the perfect case.

The effective PSF of the system, the polychromatic confocal PSF, for a particular bandwidth and pupil size, is finally obtained as the square of the corresponding polychromatic PSF obtained in a single pass:

$$ConfPSF_{Polychromatic} = \left|PSF_{Polychromatic}\right|^2. \tag{8}$$

The calculations of the previously described polychromatic confocal PSFs were accomplished by using Matlab routines, specifically developed for these particular purposes.

3. Results

3.1. Point images and modulation transfer functions

Theoretically, the optical quality of an imaging system (OCT system) can be characterized by its effective polychromatic confocal PSF. In this study it was calculated for three different cases. The first is the perfect one, corresponding to the situation where no aberrations are present, so both chromatic and monochromatic aberrations have been fully corrected. This situation serves as reference for the other cases. The second case of interest will be referred in the manuscript as the chromatic case, indicating the situation where only chromatic aberrations are present. This scenario corresponds to the condition of a hypothetical perfect monochromatic aberration correction, showing the limits and benefits of AO operating in combination with the OCT system, leaving the chromatic aberration uncorrected. This is precisely the situation of AO OCT setups recently reported [13,15,16]. Finally, aberrations obtained from real eyes, including the effects of both monochromatic and chromatic aberrations, are also analyzed in this work, referred to as the real case. This last case models the situation of an OCT apparatus without any type of aberration correction.

Figure 1 presents some estimated polychromatic confocal PSFs, showing the degradation of the point images associated with the increase of pupil size, from 1 to 8 mm diameter. In these examples the PSFs are obtained by simulating 80 nm of bandwidth (FWHM) for the emitted spectrum. The perfect situation (‘Perfect’), i.e. free of aberrations, together with two real cases (S1 and S2) calculated by using aberrations from two subjects, are depicted. All images are normalized to their maxima.

For small pupil sizes, the images estimated from real eyes resemble the ones obtained in the perfect case. In particular, Fig. 1 shows the degradation of the images, produced by aberrations, to be relatively modest up to 2 mm pupil diameter. For larger pupil sizes, the combination of both monochromatic and polychromatic aberrations in real eyes distributes the energy out of the central peak, whose diameter remains however relatively similar to the perfect case.

#8582 - $15.00 USD Received 25 August 2005; revised 23 September 2005; accepted 23 September 2005

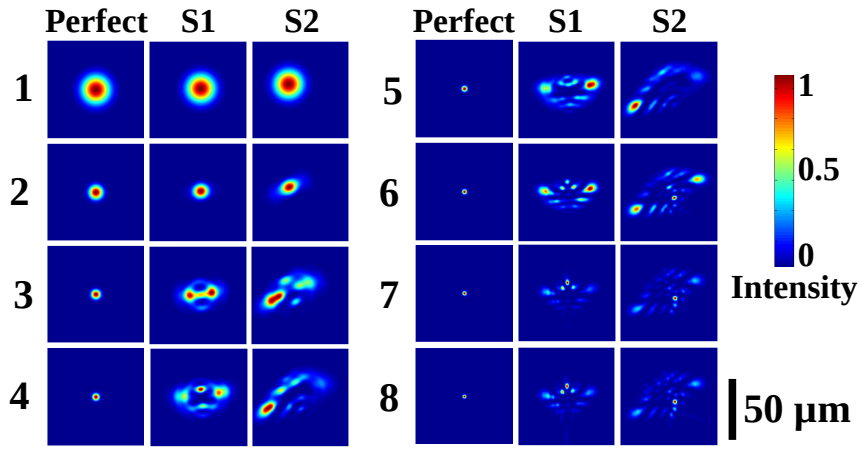

Fig. 1. Confocal polychromatic (Gaussian spectrum of 80 nm FWHM) point-spread functions obtained in the perfect case (columns 1 and 4), and for 2 subjects (S1 and S2) at different pupil sizes, ranging from 1 to 8 mm diameter. All the color-coded intensity images are normalized to their corresponding maxima. Blue color corresponds to 0 intensity while red indicates 1 (maximum intensity).

Ocular aberrations in real eyes were measured in a pupil of 8 mm. Aberrations in smaller pupil sizes were obtained numerically by multiplying the aberration maps by a circular binary mask of the required radius, and then estimating the wavefront in the new area. Figure 1 also shows, in the perfect case, that the increase of numerical aperture in the eye produced by the change in pupil size, notably affects the diameter of the point images. This effect is more pronounced in confocal arrangements as compared to the case of a single pass PSF, due to the squaring operation presented in Eq. (8).

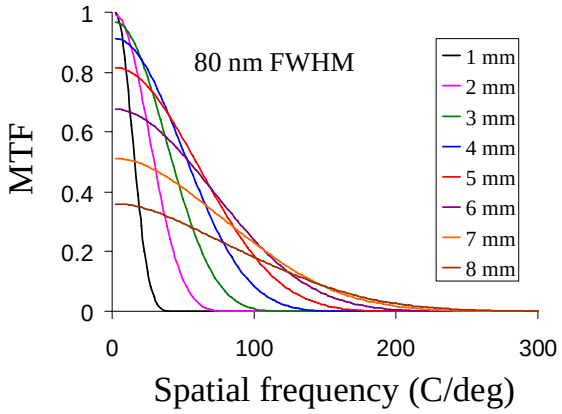

Fig. 2. Modulation transfer functions calculated in the chromatic case, assuming perfect monochromatic aberration correction, at different pupil sizes for a Gaussian optical spectrum of 80 nm FWHM.

Figure 2 presents the radial average of the modulation transfer function (MTF) associated with an 80 nm FWHM bandwidth, at different pupil sizes in the case of chromatic aberration only. MTF is calculated by Fourier transformation of the estimated confocal PSF. The cut-off frequency increases with pupil size. The maxima of the different MTF exhibit a significant decrease proportional to the pupil size. For this particular spectral bandwidth, the maxima

#8582 - $15.00 USD Received 25 August 2005; revised 23 September 2005; accepted 23 September 2005

remain within the 80 % of the perfect case up to pupils of 5 mm diameter. However, the decrease in the maxima is stronger in larger pupils: for 7 mm diameter the maximum of the MTF is reduced to 50 %, while at 8 mm the decrease is near 65 % of the peak of the ideal case. Figure 2 shows that chromatic aberration is essentially disseminating part of the energy in the tails of the point image, but keeping the width of the central peak of the PSF practically unaffected.

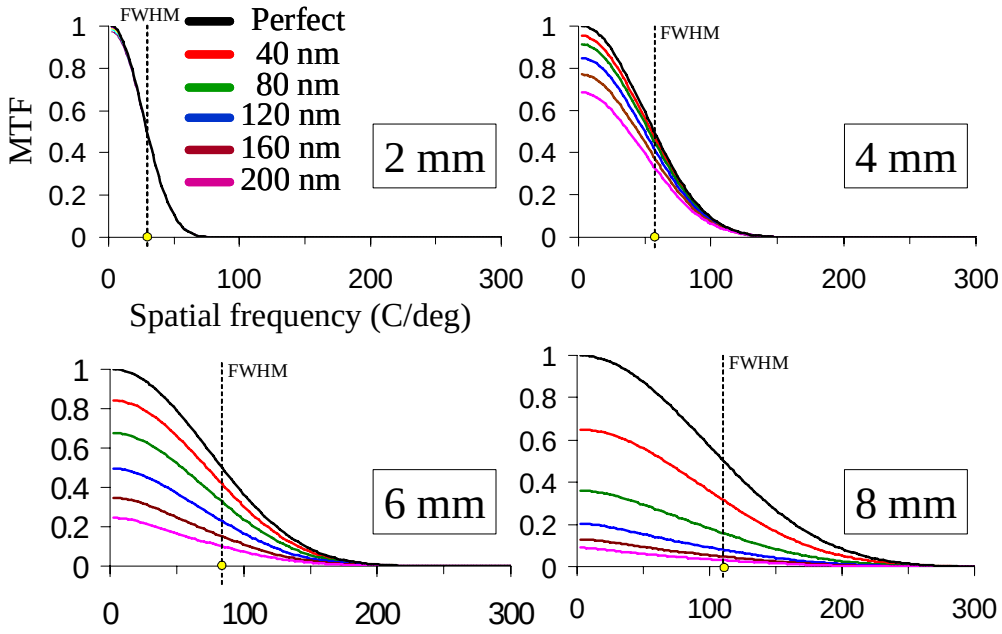

Fig. 3. Modulation transfer functions in the chromatic case, in absence of monochromatic aberrations, for different Gaussian optical spectra (indicated with different colors) and different pupil sizes. The case of perfect aberration correction is also included in black color. Dashed line shows FWHM of the MTFs.

The present simulation of this study permits to investigate and compare the effective polychromatic confocal PSF at different pupil sizes and different spectral bandwidths. Figure 3 shows the MTF for several spectral bandwidths at four selected pupil sizes: 2, 4, 6 and 8 mm diameter in the chromatic and in the perfect case. The dashed line, corresponding to the FWHM of the MTFs, shows that this parameter is independent of bandwidth for a particular pupil size, although it increases with the pupil diameter from < 50 C/deg to > 100 C/deg from 2 to 8 mm (indicated with a yellow point on axis). The graphic corresponding to the pupil of 2 mm diameter (upper left in Fig. 3) shows that the MTFs of different spectral bandwidths are very similar. Figure 3 shows that, considering a bandwidth of 120 nm, approximately the value used in ultrahigh resolution OCT, the decrease of the maximum is 15, 50 and 80 % for pupils of 4, 6 and 8 mm diameter respectively, while for pupils up to 2 mm there is practically no reduction as compared to the perfect case. The decrease is more pronounced with larger spectral bandwidths, although it is not negligible with moderate values. For instance, the decrease at a pupil of 8 mm is 40 and 60 % for bandwidths of 40 and 80 nm FWHM respectively.

3.2. Transverse resolution

Figures 2 and 3 show that the redistribution of energy in the MTF, induced by the chromatic aberration, mainly affects contrast. Contrast and resolution are not independent concepts, but on the contrary, they may provide the effective visibility of the sample in the system. In order

#8582 - $15.00 USD Received 25 August 2005; revised 23 September 2005; accepted 23 September 2005

to extract the effective resolution, contrast transfer functions will be used. Assuming two identical point objects, with their corresponding effective PSFs, contrast function presents the evolution of contrast as a function of distance between the two objects. Hence, the actual resolution can be obtained as the separation distance at which two objects are imaged with a certain value of contrast. This definition of resolution involves not only the optical properties of the system, but also might account for noise, sensitivity of the detector, etc, because the selected value of required contrast can include all these practical issues affecting the final detection of images.

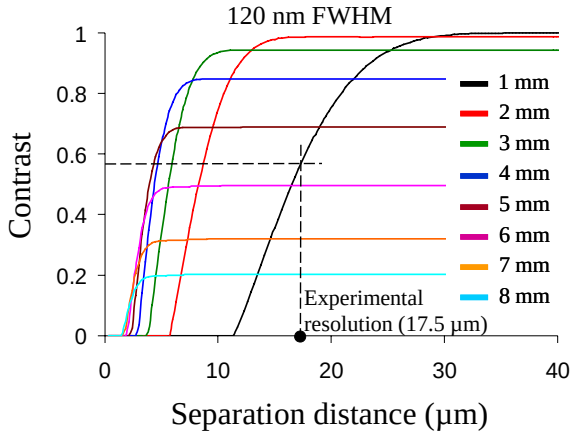

Fig. 4. Contrast functions associated with different pupil diameters obtained for a Gaussian spectrum of 120 nm FWHM (chromatic case). Experimental resolution achieved in ophthalmic OCT is shown with a dashed line.

Figure 4 depicts the contrast transfer function for different pupil sizes in the particular case of 120 nm FWHM of spectral bandwidth, resembling the situation found in ultrahigh resolution OCT. To obtain the contrast function, two identical intensity images are first generated and progressively separated by means of a Matlab routine, which simultaneously measures the contrast generated between them at every single step. The maximum contrast corresponds to the maximum of the corresponding PSF. Theoretically, if the number of photons is not limited, resolution is given by the intersection of the curves obtained for each pupil size with the separation distance axis. In the real case, noise is always present and the number of available photons and the sensitivity of the detector are limited. Hence, the resolution is no longer given by the intersection of the contrast functions with the horizontal axis, but with a line parallel to the latter instead. The value of this new reference line might include the effects of noise, sensitivity, etc. They can be either theoretically or empirically obtained. The value of the reference will indicate the contrast threshold required to resolve two identical features with the actual instrument, in this case the transverse resolution achieved in the living retina. In this work, the experimental resolution reported in most of the ophthalmic OCT setups will be adopted.

Transverse resolution is difficult to estimate in the living eye, as there is no possibility to objectively measure the true dimensions of the detected intraretinal features. Independent of the used bandwidth, transverse resolution in ophthtalmic OCT has been reported between 15 and 20 µm, using a scanning beam of 1 mm diameter [2]. As a compromise, 17.5 µm for a beam of 1 mm diameter will be used. The knowledge of the experimental resolution and pupil size, represented in Fig. 4 by dashed lines, unequivocally determines the threshold contrast. The intersection of the different curves corresponding to the different pupil diameters, at a given bandwidth, with the contrast threshold will produce the actual transverse resolution. Figure 4 shows that the maxima of the contrast functions associated with pupil sizes larger

#8582 - $15.00 USD Received 25 August 2005; revised 23 September 2005; accepted 23 September 2005

than 5 mm diameter are below the defined contrast threshold. Consequently, for the spectral bandwidth of this particular example, i.e. 120 nm FWHM, the effect of the chromatic aberration prevents the detection of signals through pupils larger than 5 mm diameter. Following the same procedure, the contrast functions are also calculated for the following spectral bandwidth: 40, 80, 160 and 200 nm.

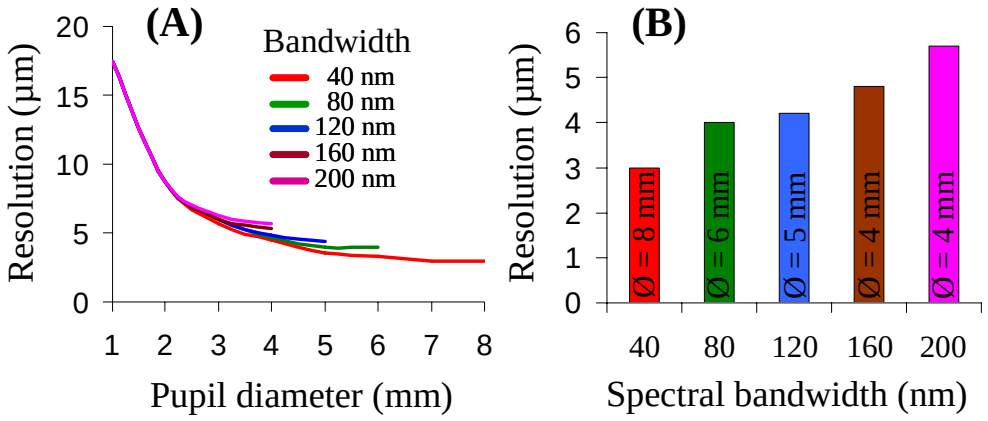

Fig. 5. (a) Resolution for different Gaussian optical spectra (indicated with different colors, showing the FWHM) as a function of the pupil size, in the case of only monochromatic aberration correction. (b) Minimum transverse resolution for different Gaussian spectra (indicated with different colors, showing the FWHM) in the case of only monochromatic aberration correction. The required pupil diameter to achieve the optimal transverse resolution is also presented for each spectral bandwidth.

Figure 5(a) depicts the transverse resolutions obtained for different spectral bandwidths. The resolutions are practically independent of the bandwidth up to a pupil of 2 mm diameter. Beyond this diameter, chromatic aberration influences the transverse resolution, increasing its effect as optical bandwidths broaden. Figure 5(a) also shows that the length of each curve associated with each spectral bandwidth is different. The contrast threshold imposes the actual limit for each bandwidth, restricting the maximum pupil size from which OCT signals can be detected. These results enable the calculation of the resolution achievable for every spectral bandwidth, assuming a perfect eye solely affected by chromatic aberration.

Figure 5(b) depicts the optimal pupil diameter, producing the optimal transverse resolution, for each spectral bandwidth. Larger pupils will not produce better transverse resolutions, but on the contrary, signals can be degraded or even disappear. This Fig. 5(b) essentially indicates that without correcting chromatic aberration present in normal eyes, the expansion of the entrance pupil of the eye may not produce the expected benefit on transverse resolution. For instance, using bandwidths broader than 120 nm, pupil size should not exceed the value of 5 mm diameter. Even for moderate bandwidths of 80 nm, the result of Fig. 5(b) shows that maximum physiological pupils should not be used, but only up to 6 mm diameter in this particular case, to improve transverse resolution.

3.3. Confocal polychromatic Strehl ratio

The possible effects of optical bandwidth and pupil size on OCT tomograms quality can also be evaluated in the case of real eyes, where chromatic and monochromatic aberrations are present. A simple and useful estimator of the optical quality is the Strehl ratio (SR), defined as the peak intensity value of the actual PSF normalized by the maximum of the PSF corresponding to the perfect case.

#8582 - $15.00 USD Received 25 August 2005; revised 23 September 2005; accepted 23 September 2005

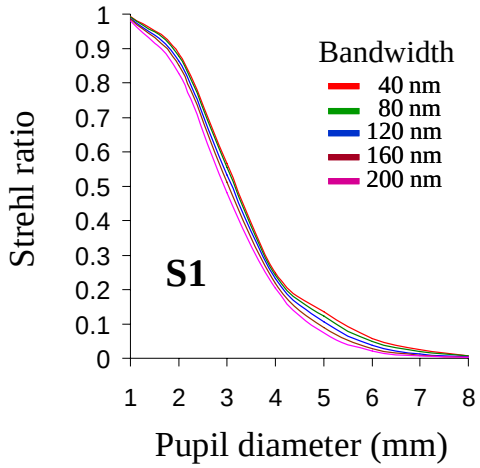

Fig. 6. Confocal polychromatic Strehl ratio calculated for Subject 1 (S1) at different spectral bandwidths as a function of the pupil diameter.

Figure 6 shows the results for subject S1. The SR decreases as a function of pupil diameter for all optical bandwidths. As expected, the maximum energy of the point images also decreases as the bandwidth increases. However, this effect is moderate. Up to 4 mm diameter in this particular subject, the curves corresponding to different spectral bandwidths evolve approximately parallel to each other. Only at 5 mm diameter, the difference between small and large optical bandwidths slightly increases. The known increase of monochromatic aberrations when increasing pupil size is interestingly balanced in the confocal case with chromatic defocus so that the combination of both keeps the maximum of the point image relatively independent of bandwidth.

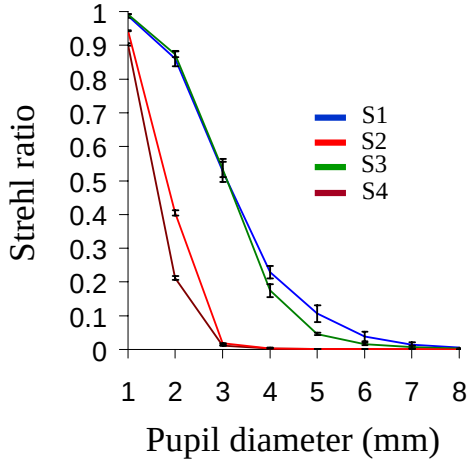

Fig. 7. Averaged confocal polychromatic Strehl ratios calculated for each subject as a function of pupil diameter.

Figure 7 shows the results for all the subjects. The data points are obtained as the mean value of the SR for different spectral bandwidths at each diameter. The error bars represent the

#8582 - $15.00 USD Received 25 August 2005; revised 23 September 2005; accepted 23 September 2005

standard deviation of the SR at the different optical bandwidths (40, 80, 120 160 and 200 FWHM). In all the cases, these errors bars are relatively small, indicating that the differences of RS among the bandwidths are modest. In absence of monochromatic aberrations, where only chromatic defocus is affecting the OCT tomogram, the results are however different.

Figure 8 shows, for each spectral bandwidth, the evolution of the SR in the chromatic case as a function of the pupil size. Increasing the bandwidth produces a significant decrease in the confocal SR, even for moderate pupil sizes. Up to 2 mm diameter, the spectral bandwidth barely affects the SR, which remains close to the ideal case (shown in Fig. 8 with dashed line). For pupils between 5 and 7 mm diameter, the slope of the curves for bandwidths larger that 40 nm is relatively similar. The average evolution obtained in the four eyes is also presented in Fig. 8 as a black line. Figure 8 indicates the benefit of an ideal, perfect monochromatic aberration correction, keeping the natural chromatic aberration uncorrected. As a possible estimation, the benefit can objectively be evaluated in terms of difference between the average curve from real eyes and the curve of particular spectral bandwidth to be used. SR does not provide direct information about the effective transverse resolution, as it has been previously described in this work. However, it shows the possible increment of the recorded signal at the detector, and it could be related with the signal-to-noise ratio of OCT tomograms. According to Fig. 8, maximum benefits are obtained over the SR when correcting monochromatic aberrations between 3.5 and 4.5 mm diameter.

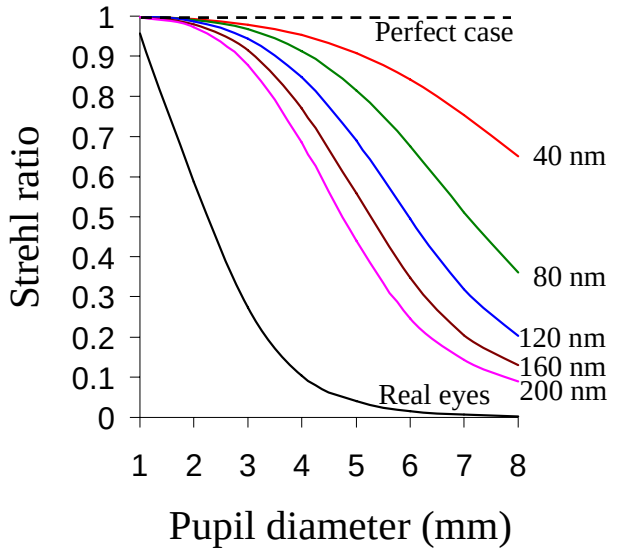

Fig. 8. Confocal polychromatic Strehl ratios at different spectral bandwidths as a function of the pupil diameter for perfect monochromatic aberration correction. The case of perfect aberration correction is presented with a dashed line. The average Strehl ratio calculated from four real eyes, including all the aberrations, is shown in black color.

4. Discussion and conclusions

In this work, optical performance of fiber optical based OCT systems has been modeled in order to study their capabilities for OCT imaging in transverse planes of the human retina. In OCT, the size of the fiber core is usually a fixed parameter. However, the assumption of confocal detection, given by the normalized radius of the fiber, is not very restrictive as it can be governed by the numerical aperture of the launching lens placed in front of the fiber. In classical confocal microscopy, the aperture size of the pinhole must often be increased to

#8582 - $15.00 USD Received 25 August 2005; revised 23 September 2005; accepted 23 September 2005

improve signal-to-noise ratio. In general, an optimum aperture size exists that maximizes signal-to-noise ratio, while still maintaining adequate signal-to-background ratio for good image contrast. The flexibility to easily change the pinhole allows to experimentally find the appropriate size. However in OCT, detailed calculations should be done during the design of the system due to the limitation of the fixed fiber core diameter according to its cut-off wavelength.

The effective transverse resolution in OCT can not fully be inferred from simple calculations solely involving the usual optical functions of the system, as the point-spread function, modulation transfer function or other related ones. Even when including the effects of chromatic aberration, these functions usually describe the performance of the system when the number of photons reaching the detector is not limited. In OCT, the rigid exposure limits required to illuminate the retina; the optical properties of the different media that light passes through in the eye, and in particular, the complexity of the intraretinal layers (presenting different reflectivity, absorption, and scattering properties) at different wavelengths, makes the use of contrast functions or similar approaches, accounting for the limited number of available photons, mandatory.

Under the premise of a well designed OCT system, we have calculated the impact of the chromatic aberration in OCT tomograms. Traditionally, efforts in ophthalmic AO have mainly focused in the measurement and correction of the monochromatic aberrations, partially leaving unattended the possible contribution of other effects, as intraocular scattering or chromatic aberrations. The magnitude of the LCA has only recently been measured and characterized systematically in the human eye [17], enabling the study of its effect for retinal imaging purposes. This is critical in AO UHR OCT, because of the mandatory and inherent use of polychromatic light sources. We have found that, in absence of monochromatic aberrations, the performance of OCT systems is limited by chromatic aberration for pupil sizes larger than 2 mm diameter. In particular, the use of larger pupil sizes in the eye to expand the numerical aperture of the system brings about the decrease of the signal at the detector, as a collateral consequence of the chromatic aberration. This effect has been proven to be noticeable even for moderate pupil sizes (4-6 mm diameter) and spectral bandwidths (80 nm FWHM). The impairment of the detected signal is dramatic when using wide pupils, in the range of 6-8 mm diameter. This is precisely the ambit where most of the ophthalmic AO system currently operate, only correcting monochromatic aberrations. It has also been shown that signal losses can be as high as ~80 % of the maximum in the particular case of UHR OCT when using 120 nm optical bandwidth at FWHM and a pupil diameter of 8 mm. The present simulation indicates that, unless chromatic aberration is corrected, the expansion of pupil in OCT to increase the transverse resolution should be conservative and always balanced with the spectral bandwidth employed.

Comparison of our results with experimental data requires careful considerations. The examination of the obtained OCT tomograms is the ultimate test to evaluate the effective experimental resolution. In this context, some recently published retinal images are available for comparison with our theoretical calculations. In Hermann *et al.* [13], partial monochromatic aberration correction in a fiber optical based UHR OCT setup was performed, using a light source emitting a Gaussian spectrum centered at 800 nm of 130 nm bandwidth at FWHM. Pupil size was limited to 3.68 mm diameter, because of the modest performance of the correcting device (electrostatic deformable mirror with 37 independent actuators). The UHR OCT retinal images show intraretinal structures, vessels and capillaries, resolved near the parafoveal region. Accounting for their location, they are known to be in the range of 5-10 μm diameter in normal retinas. This range is in agreement with the prediction of the calculations presented in this work. For a perfect monochromatic aberration correction, which was not totally accomplished in the cited work, the theoretical estimate is ~6 μm resolution. More recently, volumetric images of the living retina have been reported using a fiber optical based UHR OCT system (illuminated by Gaussian spectrum centered at 800 nm and 130 nm bandwidth FWHM) interfaced to AO, using a liquid crystal spatial light modulator as the correcting device [16]. In Fernández et al. [16], the authors hypothesize about the nature of

#8582 - $15.00 USD Received 25 August 2005; revised 23 September 2005; accepted 23 September 2005

some intraretinal features resolved in the external limiting membrane of the human retina. Accounting for the location and distribution of the structures presented in the retinal three-dimensional OCT tomograms, they are believed to correspond to clusters of terminal bars of photoreceptors, in particular rods. In this case, experimental estimation of the resolution is ~5 μm. This value is very close to the theoretically predicted in Fig. 5. An interesting fact reported in the mentioned work is the absence of increase in the signal-to-noise ratio when correcting the aberrations through a pupil of 6 mm diameter. In the simulations, Fig. 8, the loss of intensity at the maximum of the point images when using a pupil of 6 mm in combination of bandwidth 120 nm FWHM is near 50 %, while for the case of 4 mm diameter the losses are less that 20 %. The huge degradation of the signal produced by the chromatic aberration by imaging through a pupil of 6 mm could explain the lack, or reduction, of benefit when performing monochromatic aberration correction at these particular pupil size and spectral bandwidth. Other OCT retinal images obtained with AO, using a free-space interferometer, and solely correcting the ocular aberrations in a single pass, are also available in the literature, Zhang et al. [15], claiming transverse resolution of 3 μm. In the referenced work, the OCT setup is not fiber optical based, so direct comparison to the simulation of the present manuscript can not be exactly done. However, assuming a perfect confocal design (enabling higher resolution than single pass imaging or conventional imaging), and a perfect monochromatic aberration correction, the simulation indicates, accounting for the used spectral bandwidth (45 nm FWHM) and pupil diameter (6 mm), a best transverse resolution of 3.5 μm.

In summary, for UHR OCT imaging, the ideal situation would be the use of a broad spectral bandwidth light source, enabling ultrahigh axial resolution, with the simultaneous operation of the maximum physiological pupil size in the eye in combination with AO to achieve high transverse resolution. However, calculations of the present study show that this ideal scenario from the optical point of view will not produce the expected benefits but on the contrary, signal would be seriously impaired in some cases, unless chromatic aberration in the human eye is also corrected. The theoretical simulations have shown the optimal combination of bandwidth and pupil size to be used, and the expected resolution of the obtained retinal OCT tomograms. The results presented in this work can help in the design of ophthalmic OCT systems to be operated with AO.

Acknowledgments

We gratefully acknowledge P. M. Prieto and P. Artal, Laboratorio de Optica, Universidad de Murcia, and A. Unterhuber, B. Hermann, B. Povazay, Vienna University of Medicine, for their contribution to the measurement of the presented ocular aberrations. P. Artal is also acknowledged by his useful comments during preparation of the manuscript. We want to thank an anonymous reviewer for his/her suggestions, which have notably improved the quality of this work.

This research was supported in part by FWF Y159-PAT, the Christian Doppler Society, FEMTOLASERS Produktions GmbH, and Carl Zeiss Meditec AG.

W. Drexler, the corresponding author, can be reached by phone, 43-1-4277 60726; fax: 43-1-4277 9607; or e-mail, wolfgang.drexler@meduniwien.ac.at.

#8582 - $15.00 USD Received 25 August 2005; revised 23 September 2005; accepted 23 September 2005